Int. J. Dev. Biol. 60: 5-12 (2016)
doi: 10.1387/ijdb.150222cl

THE INTERNATIONAL JOURNAL OF DEVELOPMENTAL BIOLOGY
www.intjdevbiol.com

Live imaging reveals spatial separation of parental chromatin until the four-cell stage in *Caenorhabditis elegans* embryos

JITKA BOLKOVÁ and CHRISTIAN LANCTÔT*,1

Institute of Cellular Biology and Pathology, First Faculty of Medicine, Charles University in Prague, Prague, Czech Republic

ABSTRACT The parental genomes are initially spatially separated in each pronucleus after fertilization. Here we have used green-to-red photoconversion of Dendra2-H2B-labeled pronuclei to distinguish maternal and paternal chromatin domains and to track their spatial distribution in living *Caenorhabditis elegans* embryos starting shortly after fertilization. Intermingling of the parental chromatin did not occur until after the division of the AB and P1 blastomeres, at the 4-cell stage. Unexpectedly, we observed that the intermingling of chromatin did not take place during mitosis or during chromatin decondensation, but rather ~3-5 minutes into the cell cycle. Furthermore, unlike what has been observed in mammalian cells, the relative spatial positioning of chromatin domains remained largely unchanged during prometaphase in the early *C. elegans* embryo. Live imaging of photoconverted chromatin also allowed us to detect a reproducible 180° rotation of the nuclei during cytokinesis of the one-cell embryo. Imaging of fluorescently-labeled P granules and polar bodies showed that the entire embryo rotates during the first cell division. To our knowledge, we report here the first live observation of the initial separation and subsequent mixing of parental chromatin domains during embryogenesis.

KEY WORDS: *Caenorhabditis elegans, parental chromatin, live imaging, embryogenesis, photoconversion*

Introduction

Fertilization in *C. elegans* is followed by the formation of maternal and paternal pronuclei in the zygote. The main steps in this process are the decondensation of sperm and oocyte chromatin and the addition of a nuclear envelope. These steps are preceded on the maternal side by completion of both meiotic divisions and, on the paternal one, by the substitution of the putative protamines SPCH-1,2,3 for histones in the sperm chromatin (Chu *et al.*, 2006). Epigenetic changes have been reported to occur during formation of the pronuclei. For instance, the maternally derived histone variant H3.3 rapidly incorporates into both pronuclei whereas the H2A variant HTZ-1 is removed (Ooi *et al.*, 2006; Samson *et al.*, 2014). The paternal chromatin is hypoacetylated relative to the maternal one, especially at the H4K16 site, whereas the overall levels of histone methylation do not differ significantly between the two pronuclei (Samson *et al.*, 2014). Once pronuclei are formed, DNA replication is initiated and the pronuclei start their migration toward each other (Edgar and McGhee, 1988). After meeting of the pronuclei, the first embryonic mitotic division takes place, quickly followed by subsequent divisions of embryonic blastomeres in a reproducible and determined manner (Deppe *et al.*, 1978; Sulston *et al.*, 1983).

Previous work, mainly done in the mouse embryo, sought to determine the timing and the extent of intermingling of the parental genomes after their initial apposition in the zygote. Ito and colleagues treated male mice with the halogenated thymidine analog bromo-deoxyuridine (BrdU) in order to label sperm DNA (Ito *et al.*, 1988). Mating with untreated females allowed them to distinguish parental genomes in the resulting embryos. These authors found no obvious pattern in the positioning nor in the distribution of paternal DNA strands, but they mention that their results cannot exclude patterned segregation during the first few embryonic cell divisions. In a more recent and detailed study, and using a similar approach of labeling sperm DNA with BrdU,

Abbreviations used in this paper: BrdU, bromodeoxyuridine; FISH, fluorescence *in situ* hybridization, MosSCI, Mos1-mediated single copy insertion.

***Address correspondence to:** Christian Lanctôt. Institute of Cellular Biology and Pathology, First Faculty of Medicine, Charles University in Prague, Albertov 4, 128 00 Prague, Czech Republic. Tel. +420-224-968-015. Fax. +420-224-917-418. E-mail: christian.lanctot@lf1.cuni.cz; www.lanctotlab.org

1 Present address: BIOCEV- Department of Cell Biology, Faculty of Science, Charles University in Prague, Průmyslová 595, 252 42 Vestec, Czech Republic. E-mail : lanctotc@natur.cuni.cz

Supplementary Material (3 videos, 2 figures, 1 table) for this paper is available at: http://dx.doi.org/10.1387/ijdb.150222cl

Accepted: 24 September 2015

ISSN: Online 1696-3547, Print 0214-6282
© 2016 UPV/EHU Press
Printed in Spain

Mayer and colleagues concluded that the parental DNA remained clearly segregated until the four-cell stage in the mouse embryo (Mayer *et al.*, 2000b). These results were confirmed using DNA FISH to analyze the spatial distribution of the distinct centromeric sequences from each species in hybrid embryos. Interestingly, the DNA in the mouse male pronucleus was found to be actively demethylated within a few hours of fertilization, unlike what was observed in the female pronucleus (Mayer *et al.*, 2000a; Oswald *et al.*, 2000; Santos *et al.*, 2002). It has been suggested that this epigenetic asymmetry is related to the spatial segregation of the parental genomes.

In *C. elegans*, a BrdU labeling scheme was used to detect parental DNA during embryonic development (Ito and McGhee, 1987). However, in this work the emphasis was put on determining whether the labeled DNA strands co-segregated reproducibly to the same embryonic cells (which they do not); no attempt was made to investigate the mixing of paternal and maternal chromatin after fertilization. We therefore decided to study this process in the living *C. elegans* embryo. We found that the maternally- and paternally-derived chromatin did not mix until after the division of the AB and P1 blastomeres, in the 4-cell embryo. To our knowledge, we report here the first live observation of the initial separation and subsequent mixing of the parental chromatin in an early embryo.

Results

Generation and characterization of a C. elegans strain expressing a photoconvertible form of histone H2B in the germline and in early embryos

To be able to distinguish the parental genomes in the early *C. elegans* embryo, we first tried to specifically label the maternal DNA by injecting a fluorescent derivative of a nucleotide (Cy3-dUTP) into the adult gonad. In doing so, we had hoped that the label would be incorporated in the replicating DNA in the distal gonad and that the labeled DNA would eventually have ended up in the maternal pronucleus after meiosis. Although labeling of the DNA in the gonad and in the oocytes proved to be easy and efficient, we failed to obtain any significant number of early embryos in which labeled DNA could be detected, and those that did show labeled chromosomes looked abnormal (data not shown). The cause for this remains unclear, but we suspect that it might be due to the inability of Cy3-dUTP-containing maternal DNA to efficiently participate in early developmental processes. We therefore resorted to an alternative strategy to image the parental chromatin in *C. elegans*, one that is based on the expression of a photoconvertible form of histone in the germ line and on the selective photoconversion of either oocyte-derived or sperm-derived chromatin shortly after fertilization. We chose Dendra2 as a photoconvertible marker. Dendra2 is a monomeric green fluorescent protein (emission λ_{max} = 507 nm) that can be converted to a red fluorescent protein (emission λ_{max} = 573 nm) upon illumination with 405 nm light (Gurskaya *et al.*, 2006). Dendra2 protein efficiently matures at 20°C, which makes it suitable for use in *C. elegans*. A strain expressing a Dendra2::H2B coding sequence under the control of the *mex-5* promoter (-472 to +1) and fused to the *tbb-2* (β-tubulin) 3' untranslated region was obtained through insertion of the transgene at the *ttTi5605* site using the Mos1-mediated single copy insertion (MosSCI) method (Zeiser *et al.*, 2011).

Transgenic worms (strain JBL1) were imaged by selective plane illumination microscopy, which revealed the expected pattern of expression of the Dendra2-H2B fusion protein, i.e throughout the gonads (with stronger expression starting in pachytene nuclei) as well as in spermatozoa and in nuclei of the embryos in the uterus (Suppl.Video 1). Dendra2-H2B was detected in nuclei up to the L1 stage (data not shown). By illuminating a region-of-interest with

TABLE 1

PROPORTION OF CASES IN WHICH THE PATERNALLY- AND MATERNALLY-DERIVED CHROMATIN WERE OBSERVED TO BE SPATIALLY SEPARATED

	P0	AB	P1	ABa	ABp	EMS	P2
Prophase	22/22	11/11	9/10	0/7	0/6	0/11	0/8
Metaphase	26/26	7/10	10/12	0/6	0/3	0/7	0/6
Anaphase	24/24	8/11	8/10	0/7	0/7	0/6	0/6

The number of images with separated parental chromatin / total number of images is indicated. The imaging data consisted of movies and snapshots taken at various times after photoconversion of either of the pronuclei. Results are presented according to the mitotic phase (rows) and blastomere identity (columns).

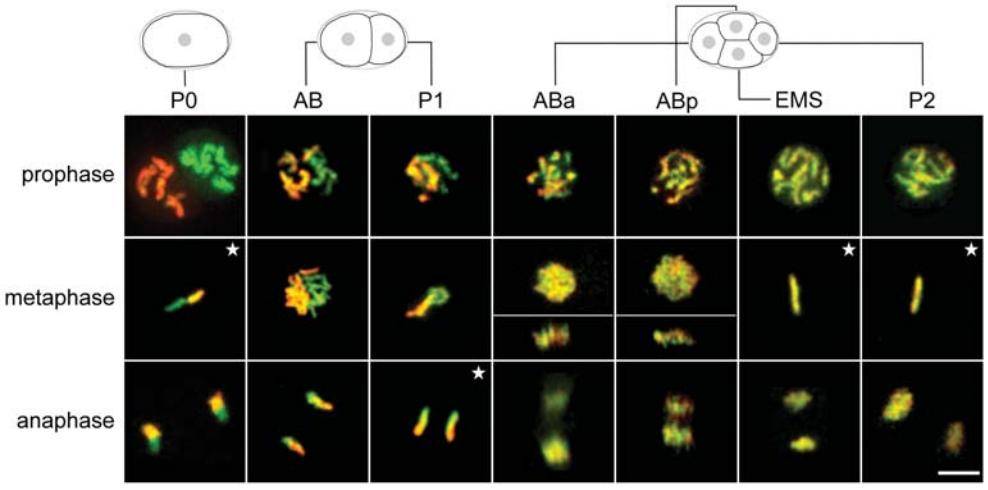

Fig. 1. Paternally- and maternally-derived chromatin remain spatially separated until the 4-cell stage. *One of the pronuclei was photoconverted in the early zygote of the Dendra2-H2B-expressing strain, after which imaging of the chromatin from the photoconverted pronucleus (red) and from the other pronucleus (green) was performed until the 4-cell stage. Representative images are taken from different embryos. Shown are maximum projections of image stacks, except for panels labeled with asterisks, which show single optical sections. Nuclei are in mitotic prophase (upper panels), metaphase (middle panels) or anaphase (lower panels). The blastomere identity is indicated and schematized on top of the corresponding panels. Note the clear separation of parental chromatin in the anaphase of AB and P1 and the mixing of chromatin (yellow) in all mitotic nuclei of the 4-cell embryo. Orthogonal views are shown for the ABa and ABp nuclei in metaphase and anaphase. Scale bar, 5 μm.*

the 405 nm diode laser (see Materials and Methods), a green-to-red photoconversion of the labeled chromatin was observed (Fig. S1). The increase in red fluorescence after photoconversion was on the order of ~100-fold (not shown). However, we noted that the green fluorescence intensity was often unchanged or only partly decreased after photoconversion. Our attempts to reach a higher proportion of photoconverted molecules (i.e. a larger decrease in green fluorescence) by increasing laser power only led to overall bleaching of both signals. It should be noted that the residual green fluorescence we observed after photoconversion did not hinder our ability to perform the analyses that are described below. Actually, the biggest problem we faced while imaging Dendra2-H2B-expressing embryos was the high photosensitivity of the fluorescent fusion protein.

The paternal and maternal chromatin remain separated until after the division of the AB and P1 blastomeres

The strategy we used to follow the spatial distribution of parental chromatin in the early embryo was to specifically photoconvert the chromatin of either the paternal or maternal pronucleus at a time when they were still well separated in the zygote. The maternal pronucleus was identified as the closest to the polar bodies. To assess the phototoxicity of the 405 nm laser line, we first subjected young embryos (< 50-cell stage) to our photoconversion protocol and tested whether they could develop into larvae. Out of 23 that were treated, 22 proceeded to hatch normally. To investigate the issue of phototoxicity in the zygote, we photoconverted the chromatin in one of the pronuclei and imaged the subsequent steps of embryogenesis. The time at which the metaphase plate was observed in the 1-cell embryo was taken as a reference point. The time to the next metaphase was measured for each blastomere. Although there was a trend toward a slight delay in cell division after photoconversion, i.e. 14.0 ± 1.0 minutes for the AB cell in irradiated embryos vs. 13.1 ± 0.4 minutes in control embryos, the differences were not highly significant ($p = 0.0681$, Mann-Whitney test, Supplementary Table 1). Taken together, our results show minimal phototoxicity during photoconversion of the Dendra2-H2B-expressing worm embryos.

The efficiency of photoconversion was similar for male and female pronuclei, and the results were similar irrespective of which pronuclear chromatin was photoconverted. After photoconversion, imaging of green and red fluorescence was performed at high speed and in three dimensions on a confocal spinning disk microscope. Similar results were observed in interphase and mitotic embryonic nuclei. However, because the accompanying condensation of chromatin led to stronger fluorescence signals, the spatial distribution of parental chromatin could be most clearly seen in mitotic nuclei (Fig.1). We observed well-defined separation of the paternal and maternal chromatin in zygotes and in two-cell embryos (Suppl. Video 2). In the latter, the chromatin was spatially segregated according to parent-of-origin in both the AB and P1 blastomeres. It was only after the division of these blastomeres that extensive intermingling of the parental chromatin occurred. This was most clearly seen on mitotic figures of 4-cell embryos. We did not observe any change in the relative spatial distribution of the parental chromatin domains during the rotation of the P1 blastomere.

The spatial distributions of parental chromatin in early blastomeres, as observed in a total of 38 movies, are summarized in Table 1. Except for cases where the Dendra2-H2B signal was too weak to conclude without any doubt, the maternal and paternal chromatin were observed to be spatially segregated in the zygote

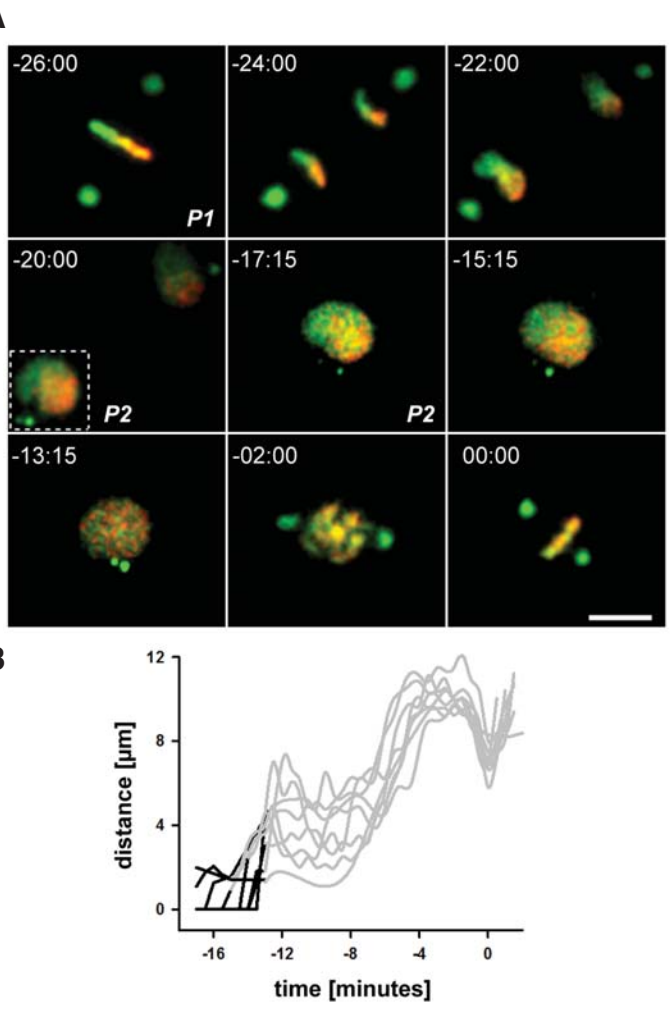

Fig. 2. Spatial redistribution of chromatin occurs shortly after cell division. *Half of the chromatin in the nuclei of P1 was photoconverted during metaphase and subsequently imaged until the next metaphase, which was taken as a reference time point (0:00). The strain that was used (JBL2) expresses Dendra2-H2B and γ-tubulin-GFP to label both chromatin (green and red) and centrosomes (green).* **(A)** *After photoconversion, the chromatin domains remain spatially segregated throughout the remainder of mitosis (e.g. time -22:00), during chromatin decondensation (e.g. time -20:00) and during the first minutes of the next cell cycle (time -15:15). The intermingling of the chromatin domains occurs relatively abruptly (at time -13:15 in the image sequence that is shown). Shown are maximum projections corresponding to cross-sections of the embryonic nuclei of 1.5-5 µm. Time is indicated in minutes:seconds. Scale bar, 5 µm.* **(B)** *Starting after the completion of the P1 division, the spatial distribution of the differently-labeled chromatin domains was assessed in the P2 nucleus at intervals of 0.5 to 2 minutes and scored either as spatially segregated or mixed. The score is plotted against the time relative to the P2 metaphase (on the x-axis, 0:00 represents the occurrence of this metaphase) as well as the actual cell cycle progression indicated by the distance between the centrosomes (on the y-axis). The spatially segregated phenotypes (black portion of the plots, n = 8) are observed at the beginning of the cell cycle, but not later than 5 minutes into the cell cycle. The chromatin domains are clearly mixed (gray portion of the plots) when the two centrosomes begin to rapidly move away from each other (time point -6:00).*

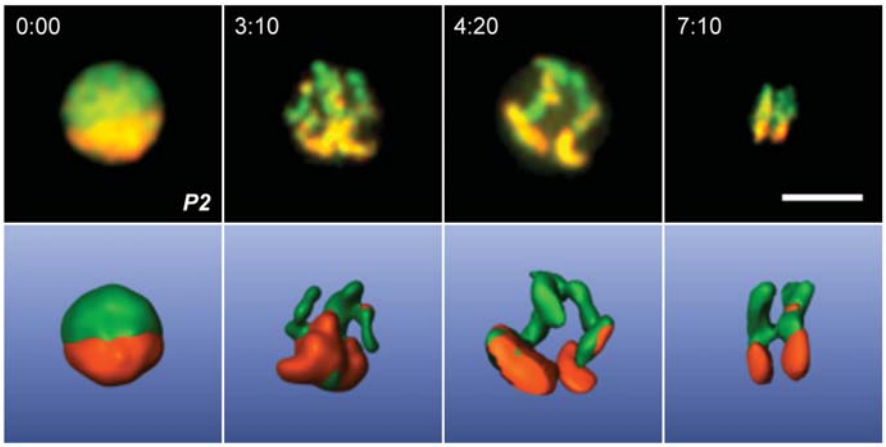

Fig. 3. The relative spatial distribution of chromatin is largely maintained during mitosis. *The chromatin in half of the P2 nucleus of a strain expressing Dendra2-H2B (JBL1) was photoconverted during S phase (time 0:00). Image stacks were acquired during the subsequent mitosis. Shown are representative maximum projections of image stacks acquired from prophase to anaphase (top panels) as well as the corresponding 3D reconstructions (bottom panels). Note that the spatial distribution of the photoconverted chromatin is largely maintained during mitosis (compare first and last time points). Time is indicated in minutes:seconds. Scale bar, 5 μm.*

(34/34 cases) and in the 2-cell embryo (12/14 cases), but never at the late 4-cell stage (0/14 cases). It could be argued that the intermingling we observed is not the result of chromatin movement, but rather of the exchange of histone H2B molecules between the photoconverted and the non-photoconverted chromatin domains. We believe this to be unlikely because the half-time for histone H2B exchange is on the order of hundreds of minutes (Kimura and Cook, 2001), i.e. much longer than the entire sequence of events that are imaged in the present work.

To determine whether one of the parental chromatin domains adopted a reproducible position relative to the future dorsoventral axis, either the maternal or paternal pronucleus was photoconverted and development was then imaged up to the 4-cell stage, at which point the dorsoventral orientation of the embryo could be determined from the position of the ABp cell on the dorsal side (Singh and Pohl, 2014). Looking back in time, the position of the labeled chromatin domain was determined in the same embryo at the 2-cell stage. No obvious bias was found in the positioning of the parental chromatin domains along the future dorsoventral axis.

The mixing of spatially separated chromatin occurs shortly after chromatin decondensation within the first minutes of the cell cycle at the 4-cell stage

Our efforts to determine more precisely the time at which the mixing of parental chromatin occurred proved unsuccessful because the progressive loss of signal intensity from the photoconverted Dendra2-H2B molecules prevented us from distinguishing unambiguously the parental chromatin signals during the interphase of 4-cell embryos. This loss in signal intensity was likely due to a combination of photobleaching and dilution through cell division. To counter this technical limitation, we decided to photoconvert half of the metaphase plate of a dividing blastomere of the 2-cell embryo, thus recreating the segregated chromatin pattern that had been observed in previous experiments. We then followed the respective movement of photoconverted and non-photoconverted chromatin at high temporal resolution. These experiments were carried out in the P1 cell since this blastomere divides more or less parallel to the imaging plane, which allows for higher resolution than if the cell divides along the z axis, as does the AB cell. As shown on Fig. 2A, we did not observe any obvious change in chromatin distribution during chromatin decondensation after division of P1. In fact, the chromatin that had been photoconverted in half of the P1 metaphase plate remained mainly confined to half of the daughter nucleus within the first minutes after cell division. After that time, the photoconverted chromatin intermingled rather rapidly with the non-photoconverted chromatin. The mixing of the differently labeled chromatin domains was clearly observed in the subsequent mitotic stages.

To quantify these observations and to determine more precisely the timing of chromatin intermingling, we took advantage of the fact that the strain that was used expressed both Dendra2-H2B and γ-tubulin-GFP, a marker of the centrosomes. The number and position of the centrosomes was used to assess the actual stage of the cell cycle in the daughter P2 cell. Since the start of image acquisition was not precisely synchronized after the photoconversion of half of the P1 metaphase, the occurrence of the subsequent metaphase was used as a reference time point. A total of 10 movies were made, 2 of which could not be used either because of high photobleaching or because of aborted cell cycle. Images from the others (n = 8) were analyzed and the degree of mixing was

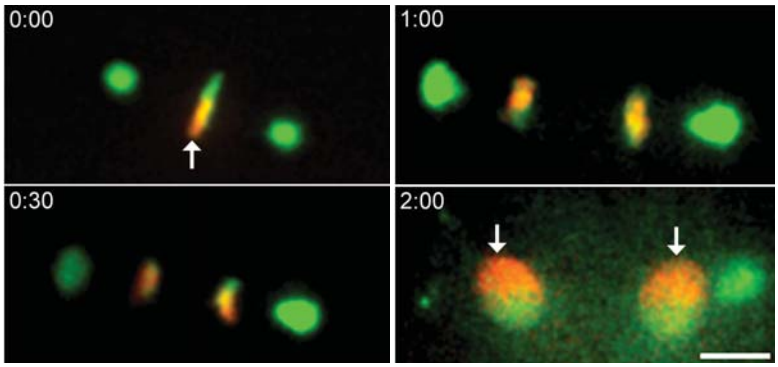

Fig. 4. The chromatin rotates by 180° during the division of the one-cell embryo. *The male pronucleus was photoconverted shortly after fertilization in the JBL2 strain, which expresses Dendra2-H2B and γ-tubulin-GFP to label both chromatin (green and red) and centrosomes (green). Imaging began at metaphase shortly after pronuclear fusion (time 0:00). Starting in late anaphase and continuing during telophase (time points 0:30 and 1:00), the nascent nuclei rotate by 180°, such that the photoconverted chromatin is found at the 2-cell stage on the opposite side relative to its initial position (compare the direction of the arrows at the first and last time points). Shown are maximum projections corresponding to a cross-section of the embryo of 6.5-10 μm. Time is indicated in minutes:seconds. Scale bar, 5 μm.*

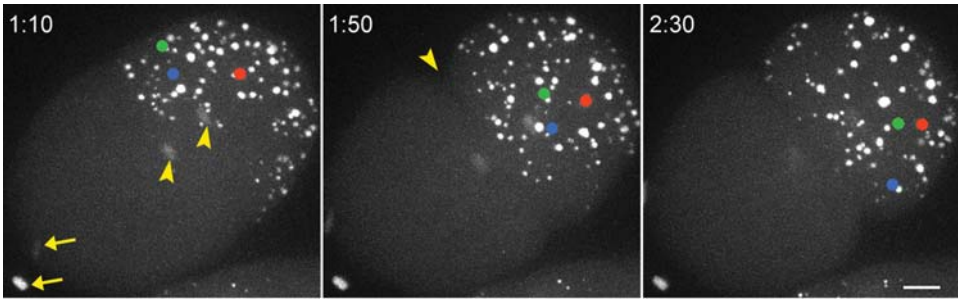

Fig. 5. The cytoplasmic P granules rotate during cytokinesis of the *C. elegans* zygote. *A strain expressing Dendra2-H2B and GFP-labeled PGL-1, a marker of P granules, was imaged at 10-second intervals. Shown are maximum projections of image stacks of part of the embryo (20 μm) at 3 different time points. Colored dots mark three individual P granules, which are clearly seen to rotate around the anterior-posterior axis during cell division. In the left panel, the Dendra2-labeled chromatin in the nascent nuclei (arrowheads) and in the polar bodies (arrows) is indicated. The arrowhead in the middle panel (time 1:50) labels the asymmetrically-forming cytokinetic furrow. Time is indicated in minutes:seconds after the start of imaging. Scale bar, 5 μm.*

plotted relative to the actual time and to the distances between centrosomes (Fig. 2B). The first occurrence of mixing occurred 4 ± 1 minutes after the beginning of the cell cycle, 2 ± 1 minutes after the appearance of two distinct centrosomes, presumably at the beginning of S phase, and 6 ± 1 minutes *before* one of the centrosomes started to migrate toward the opposite pole upon mitotic entry. Taken together, these observations indicate that the intermingling of chromatin in the early *C. elegans* embryo does not occur during chromatin decondensation at the end of mitosis, but relatively abruptly 3-5 minutes into the cell cycle, well before one of the duplicated centrosomes begins to migrate toward the opposite side of the nucleus.

The relative spatial distribution of chromatin is largely maintained throughout mitosis in the early C. elegans embryo

The preceding results did not exclude the possibility that the mixing of chromatin domains might occur prior to formation of the metaphase plate, as was previously observed in mammalian cells (Strickfaden *et al*., 2010). To investigate this issue in the early *C. elegans* embryo, the chromatin in half of a nucleus at the 2- or 4-cell stage was photoconverted during S phase and chromatin distribution was followed throughout the subsequent mitosis. As shown on Fig. 3, no drastic change in relative chromatin distribution was observed at any time during mitosis. This behavior was observed in 8 out of 11 experiments.

Chromatin rotates around the anterior-posterior axis during the first embryonic division

In the course of this study, we noticed a reproducible rotation of the one-cell embryo chromatin around the anterior-posterior axis (Fig. 4 and Suppl. Video 2). The observation was made on 16 out of 18 embryos that were analyzed. We were able to detect this intriguing movement thanks to the property of Dendra2, which allowed us to visualize a reproducible spatial pattern on the metaphase plate of the one-cell embryo as a consequence of the earlier photoconversion of one of the pronuclei. The rotation of the chromatin, which was not observed at later stages, started in anaphase of the one-cell embryo and was completed by late telophase. The orientation of the rotation was right-handed around the anterior-posterior axis, meaning that if the thumb is pointing toward the posterior, the fingers point the direction of rotation. The handedness of the rotation did not depend on which of the pronuclei was photoconverted. The rotation described half a turn (180°) and was completed within about 1 minute.

To assess whether the rotational movement that we observed was limited to the nascent nuclei or whether it concerned other embryonic structures as well, we imaged the behavior of the cytoplasmic P granules at the time of chromatin rotation. These were labeled with a GFP-PGL-1 fluorescent fusion protein (Gallo *et al*., 2010). Images were acquired in 3D at 10-second intervals from metaphase until the one-cell embryo had divided. We observed a clear rotation of the P granules (in 8 out 8 cases, Fig.5 and Suppl. Video 3). Like the chromatin, the P granules were found to rotate in a right-handed direction on the anterior-posterior axis and with an apparent angle of about 180°. The duration of rotation was longer for P granules (~3 minutes) than for the chromatin (~1 minute). The tracking of Dendra2-H2B-positive polar bodies provided additional information on movement of the embryo. The first polar body did not move. However, the second polar body, which unlike the first one is attached to the plasma membrane (Benenati *et al*., 2009), underwent an obvious rotation. Taken together, these results suggest that the entire one-cell embryo rotates inside the egg shell during cytokinesis. Importantly, we observed that the initiation of this rotational movement coincided with the asymmetric invagination of the cleavage furrow (on the presumptive left side of the embryo).

Discussion

Using photoconversion of Dendra2-labeled histone H2B in either pronuclei of the *C. elegans* zygote, we have been able to observe, to the best of our knowledge for the first time, the mixing of parental chromatin in living embryos. A previous work which used BrdU labeling of sperm DNA and immunodetection on fixed samples to follow the paternal genome throughout embryogenesis found that the parental DNA strands segregate randomly during development, but did not address the issue of genome mixing in the early embryo (Ito and McGhee, 1987). We now report that the parental chromatin remain spatially separated until after the second division of embryonic blastomeres, i.e. until the 4-cell stage. In separate experiments, we unexpectedly found that the intermingling of chromatin domains does not take place during mitosis as previously reported in cultured mammalian cells (Strickfaden *et al*., 2010) or during chromatin decondensation at the end of telophase. Rather, live imaging of chromatin domains through an entire cell cycle in the P1 and P2 blastomeres revealed that mixing occurs ~3-5 minutes into the cell cycle. Despite the variability we observed, it is clear from our results that 1) the chromatin domains remain spatially segregated until the appearance of two distinct centrosomes, presumably at the beginning of S phase and 2) the chromatin domains have completely mixed well before the start of the rapid movement of one of the centrosomes upon mitotic entry. The results reported here are schematized on Fig. 6.

Our observations raise a number of questions, in particular as to why the mixing of parental chromatin does not occur earlier. With regard to the zygote, the answer is simple: the contents of the pronuclei are prevented from mixing by a nuclear envelope that stays intact until the formation and alignment of individual metaphase plates in each of them (Gorjánácz and Mattaj, 2009). The rapid and directed movements of chromosomes during the subsequent anaphase are not expected to be compatible with chromatin mixing. It is not clear, however, why the parental chromatin compartments remain segregated in the AB and P1 blastomeres once zygotic division has been completed. It could be that an active mechanism prevents chromatin mixing in the 2-cell embryo, possibly based on epigenetic modifications. However, although there have been reports of differences in post-translational modifications of histones between the paternal and the maternal pronuclei, in particular the lack of H3K79me3 and H4K16Ac in paternal chromatin, these tend to be rapidly equalized, such that parental-specific histone modifications have yet to be observed at the 2-cell stage (Samson *et al.*, 2014). Whatever the molecular mechanisms that are at work, it seems clear that a temporal window has to open in order for parental chromatin mixing to occur. Since chromatin mobility has been found in mammalian cells to be constrained during S phase (Walter *et al.*, 2003) and since we show here that, to a large extent, the spatial arrangement of chromatin is maintained during mitosis in the early *C. elegans* embryo, then we hypothesize that in this organism the length of time that separates chromatin decondensation after mitosis from the initiation of S phase (i.e. the G1 phase) is a key determinant in the process of parental chromatin mixing. In this regard, it is worth noting that a progressive lengthening of the cell cycle, which affects all lineages, has been observed during the embryogenesis of *C. elegans* (Bao *et al.*, 2008). Although it is generally thought that this lengthening is solely due to longer S phases in the early embryo, with gap phases only appearing at later time points (Kipreos, 2005), the initiation of DNA replication has not yet been imaged in the living 4-cell embryos and the appearance of a brief G1 phase at this stage cannot be excluded. We therefore suggest that it is during or shortly after this brief putative G1 phase that the spatial intermingling of parental chromatin takes place inside the cell nucleus. This interpretation is consistent with previous results which showed that chromatin mobility in mammalian cells is higher in early G1 than in the remainder of the cell cycle (Thomson *et al.*, 2004; Walter *et al.*, 2003). It should be noted here, however, that the presence of a putative G1 phase may not be sufficient to account for the timing of chromatin mixing. In the mouse, the parental genomes were found to be spatially segregated in the 2-cell embryo despite the fact that the blastomeres remain in G1 for several hours at this stage (Mayer *et al.*, 2000b). Hence, additional work is needed to elucidate the mechanism of chromatin mixing. The use of a well-characterized forward and reverse genetics model such as *C. elegans* may prove helpful in this regard.

The use of a photoconvertible form of histone H2B expressed in the germ line allowed us to make additional observations on the behavior of chromatin in the early *C. elegans* embryo. As

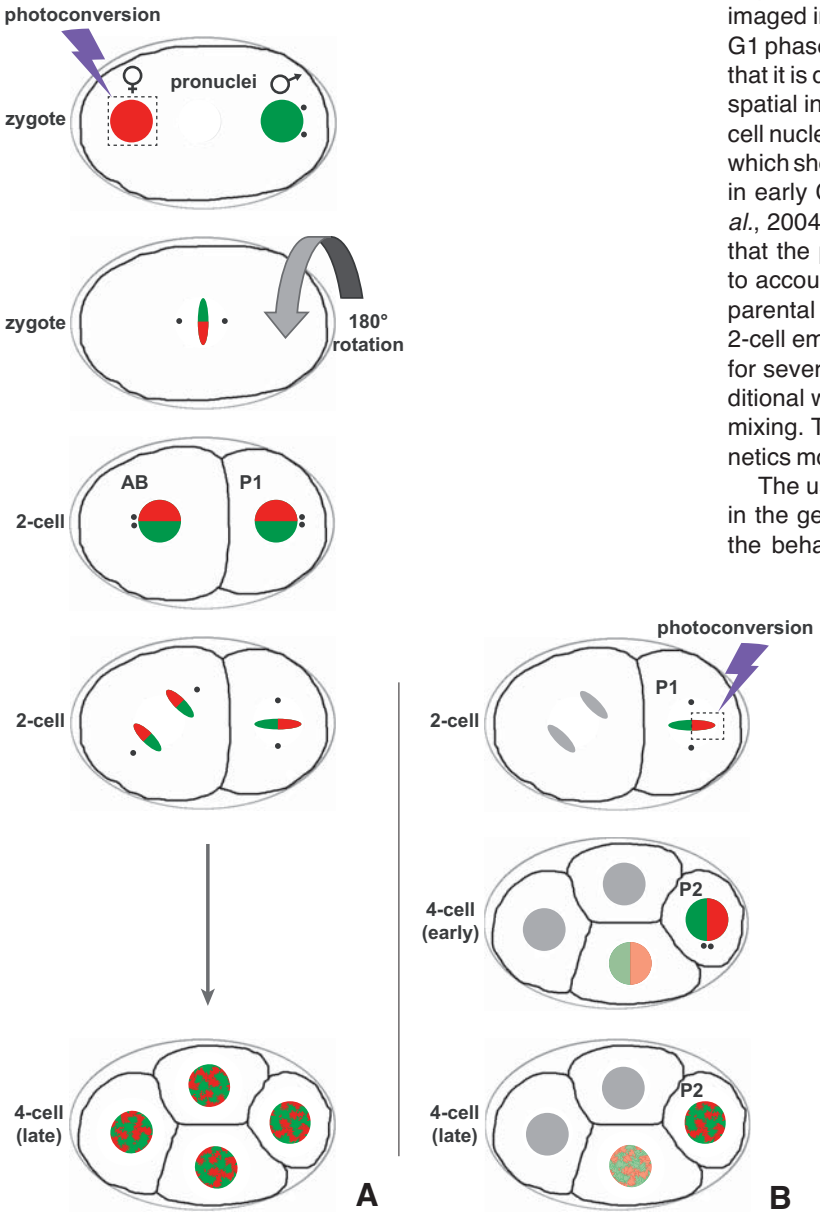

Fig. 6. Schematic representation of parental chromatin mixing in the early *C. elegans* embryo. (A) *The generation of a worm strain expressing Dendra2-H2B in the germline allowed us to specifically label the chromatin of either the male or female pronucleus through photoconversion. Live imaging of the subsequent development showed that the parental chromatin domains remain spatially segregated in the zygote and at the 2-cell stage. It is only at the late 4-cell stage that the parental chromatin domains are found to be intermingled. Photoconversion of pronuclear chromatin also enabled us to observe a reproducible 180° rotation of the whole embryo during the division of the zygote.* **(B)** *To determine more precisely the timing of chromatin mixing, differently-labeled chromatin domains were generated by photoconverting half of the metaphase plate of the P1 blastomere at the 2-cell stage. Subsequent imaging revealed that the chromatin domains remained spatially separated early after division. Mixing occurred ~3-5 minutes into the cell cycle and was complete before the start of migration of one of the centrosomes. For technical reasons, these imaging experiments were preferentially carried out on the P1 and P2 blastomeres. The chromatin domains are colored in green and in red. The centrosomes are shown as small black dots.*

mentioned above, unlike what has been reported in cultured mammalian cells, where extensive rearrangements of chromatin positioning were observed during prometaphase (Strickfaden *et al*., 2010), we did not detect a significant redistribution of labeled chromosomes relative to each other at this stage of mitosis in *C. elegans* embryos. The cause for this difference remains to be investigated. However, it is tempting to speculate that it is related to the late disassembly of the nuclear envelope and lamina during mitosis in the early (< 30-cell stage) *C. elegans* embryo (Lee *et al*., 2000), and that the maintenance of these nuclear structures until early anaphase may somehow limit and direct the movement of chromatin.

The second observation we made is that the chromatin masses undergo a reproducible rotation starting in late anaphase during the division of the zygote. Imaging of the P granules and the second polar body revealed that it is the entire embryo which is rotating inside the egg shell. The sense of the rotation along the anterior-posterior axis was found to always be the same. Similar observations were made in a recent work using cortical granules and NMY-2-GFP as fiducial markers (Schonegg *et al*., 2014). The authors of this study took the invariant sense of the rotation to indicate the intrinsic chirality of components within the one-cell embryo. They further suggested that this chirality could provide cues to establish left-right asymmetry at later stages. Interestingly, whereas the cortical granules were observed to rotate by an angle of ~120°, the nascent nuclei were found to do so by approximately half a turn (180°). This discrepancy remains to be explained; the possibility of differential rotation of organelles within the embryo deserves to be explored, in particular with regard to the nucleus, as it could represent a mean to change their cytoplasmic environment.

In summary, we have imaged the distribution of paternal and maternal chromatin relative to each other in the early living *C. elegans* embryonic nuclei. We found that intermingling of the parental chromatin first occurs in what we suggest is a brief G1 phase in the blastomeres of the 4-cell embryo. The Dendra2-H2B-expressing worm strain that we generated should prove useful in future studies on cell lineages, chromatin mobility, and histone dynamics.

Materials and Methods

Construction of a Dendra2-H2B expression cassette and insertion into a MosSCI vector

A plasmid comprising an 852 bp synthetic Dendra2 sequence that has been codon-optimized for expression in *C.elegans* (Fig. S2) and that contains 3 short introns was obtained from IDT-DNA (Iowa, USA). This sequence was PCR amplified using *AttB*-containing primers (forward 5'-ggggacaagtttgtacaaaaaagcaggctcaaaaatgaacaccccaggaatcaacc-3'; reverse 5'-ggggaccactttgtacaagaaagctgggtttacccgggccaaacttgggatg-caagtgg-3') and cloned in the Gateway pDONR221 plasmid using the BP Clonase enzyme mix (Life Technologies, CA, USA). The resulting plasmid is called CL31. A 386 bp fragment encoding a histone H2B (*his-66*) was amplified from *C. elegans* genomic DNA using primers 5'-tcagctgcaggaggttc-tatgccaccaaagccatctgcc-3' (forward) and 5'-cttgctggaagtgtacttggtaacggc-3' (reverse) and cloned in-frame at the C-terminus of Dendra2 in the unique SmaI site of CL31. The resulting plasmid is called CL33. The Gateway donor vectors containing *Ce-Dendra2* (CL31) or *Ce-Dendra2-his-66* (CL33) were sequence verified. CL33 was included along with pCFJ150 (a gift from Erik Jorgensen; Addgene # 19329; (Frokjaer-Jensen *et al*., 2008)), pCM1.36 (a gift from Geraldine Seydoux; Addgene # 17249) and pJA252 (a gift from Julie Ahringer; Addgene # 21512; (Zeiser *et al*., 2011)) in a 4-way recombination reaction catalyzed by LR Clonase II Plus (Life technologies, CA, USA) in order to generate a *Pmex-5::Dendra2::his-66::tbb-2 3'* expression cassette flanked by the *unc119* positive selection marker and left and right recombination arms for Mos1 site ttTi5605 on chromosome II.

Generation of worm strains by Mos1-mediated single copy insertion (MosSCI)

C. elegans was maintained according to standard procedures (Stiernagle, 2006). Transgenic worm lines were generated using the MosSCI transgenesis method according to published protocols (http://www.wormbuilder.org/). Briefly, the expression vectors for 1) Dendra2-H2B (25 ng/μl); 2) the Mos recombinase (pCFJ601, 50 ng/μl, Addgene # 34874); 3) the co-injection markers (pCFJ90, 1.5 ng/μl, Addgene # 19327; pCFJ104, 7.8 ng/μl, Addgene # 19328; pGH8, 7.2 ng/μl, Addgene # 19359); and 4) a heat shock-inducible negative selection marker (pMA122, 10 ng/μl, Addgene # 34873) were microinjected in L4 and young adult Unc- worms from the EG6699 Mos1 insertion strain. All Addgene plasmids were gifts from Erik Jorgensen (Frokjaer-Jensen *et al*., 2008). After injection, worms were maintained at 25°C on OP50. Heat-shock was performed at 34°C for 2 hours ~10 days after injection. Unc+Cherry- worms were screened for the presence of a Dendra2-H2B signal in the gonads on an inverted microscope. The resulting transgenic strain was extensively characterized by PCR to ascertain insertion site. Homozygotes arose spontaneously and were backcrossed twice with the wild type N2 strain. The resulting strain is referred to as JBL1 [*Pmex-5*::*Dendra2*::*his-66*::*tbb-2 3´UTR*]. JBL1 was crossed with TH27 [*tbg-1*::*gfp*] or JH2108 [*Pie-1p*::*gfp*::*pgl-1*::*pgl-1 3´UTR*] to obtain strains JBL2 and JBL3, respectively.

Imaging of Dendra2-H2B-expressing worms by selective plane illumination microscopy

Adult worms were picked and transferred to 10 μl of 0.5 mM levamisole in M9 buffer. Two hundreds μl of 1% prewarmed low-melting point agarose was added. The resulting solution was mixed, aspirated into a glass capillary and left to solidify. The capillary was mounted in the chamber of a Zeiss Z.1 light sheet microscope filled with water. Imaging was done at room temperature with a 20X water objective (NA 1.0). The long axis of the worm was approximately parallel to the light sheet and optical sections (~80 in total) were acquired with a z-step of 2 μm.

Live imaging of early embryos, photoconversion, image processing

Embryos were dissected in Early Embryo Dissection solution (EED: 4% sucrose in 0.1 M NaCl) and mounted on an agarose pad (2% in EED). Samples were then covered with an 18 mm x 18 mm coverslip (thickness 170 ± 5 μm), which was fixed to the microscope slide with candle wax. Mineral oil was pipetted around the agarose pad to prevent drying of the embryos. Imaging was done at room temperature on an Olympus IX81 inverted microscope equipped with an Andor Revolution spinning disc system and a FRAPPA module (Andor, Belfast, United Kingdom). Samples were viewed with a 100X oil immersion objective (NA 1.40). Excitation light at 488 nm or 561 nm was provided by diode lasers set at powers of 5-7.5 mW (10-15% of maximum power) and 10-12.5 mW (20-25% of maximum power), respectively. Three dimensional stacks of images (*xy* pixel size of 133 nm) were acquired with a z-spacing of 0.5 μm. Exposure to an Andor iXon Ultra 897 EMCCD camera lasted from 150-250 ms per optical section. Photoconversion was achieved in a region-of-interest (typical size of ~ 5 μm x 5 μm) with the 405 nm diode laser set at a power of 4 mW (4% of maximum power) and a pixel dwell time of 40 μs for 5 repeats. Image stacks were processed, pseudo-colored and merged using ImageJ (http://imagej.nih.gov/ij/index.html). The distances between the two centrosomes were calculated from the *xyz* coordinates of the intensity centers of the γ-tubulin-GFP signals. The distance was set at 0 μm when only one signal was detected. The extent of chromatin intermingling was assessed visually, based on the volume of the 'red' domain, i.e. the domains were considered to be spatially separated if the photoconverted chromatin occupied half of the nuclear volume or less. Otherwise, the domains were considered to

be intermingled. Three dimensional reconstructions of image stacks were performed using the Amira_6.0 software from FEI.

Acknowledgements

We thank Zdeněk Švindrych and Guy Hagen for help with microscopy. We gratefully acknowledge the financial support of the Czech Science Foundation (grants P305/12/1246 and P302/12/G157). This work was also partially supported by Charles University in Prague (PRVOUK P27/LF1/1). The Imaging Center at our institute is supported by the European Regional Development Fund (OPPK CZ.2.16/3.1.00/24010). Some worm strains were provided by the CGC, which is funded by the US NIH Office of Research Infrastructure Programs (P40 OD010440).

References

BAO Z, ZHAO Z, BOYLE T J, MURRAY J I and WATERSTON R H (2008). Control of cell cycle timing during *C. elegans* embryogenesis. *Dev Biol* 318: 65-72.

BENENATI G, PENKOV S, MÜLLER-REICHERT T, ENTCHEV E V and KURZCHALIA T V (2009). Two cytochrome P450s in *Caenorhabditis elegans* are essential for the organization of eggshell, correct execution of meiosis and the polarization of embryo. *Mech Dev* 126: 382-393.

CHU D S, LIU H, NIX P, WU T F, RALSTON E J, YATES J R 3RD and MEYER B J (2006). Sperm chromatin proteomics identifies evolutionarily conserved fertility factors. *Nature* 443: 101-105.

DEPPE U, SCHIERENBERG E, COLE T, KRIEG C, SCHMITT D, YODER B and VON EHRENSTEIN G (1978). Cell lineages of the embryo of the nematode *Caenorhabditis elegans*. *Proc Natl Acad Sci USA* 75: 376-380.

EDGAR L G and MCGHEE J D (1988). DNA synthesis and the control of embryonic gene expression in *C. elegans*. *Cell* 53: 589-599.

FROKJAER-JENSEN C, DAVIS M W, HOPKINS C E, NEWMAN B J, THUMMEL J M, OLESEN S P, GRUNNET M and JORGENSEN E M (2008). Single-copy insertion of transgenes in *Caenorhabditis elegans*. *Nat Genet* 40: 1375-1383.

GALLO C M, WANG J T, MOTEGI F and SEYDOUX G (2010). Cytoplasmic partitioning of P granule components is not required to specify the germline in *C. elegans*. *Science* 330: 1685-1689.

GORJÁNÁCZ M and MATTAJ I W (2009). Lipin is required for efficient breakdown of the nuclear envelope in *Caenorhabditis elegans*. *J Cell Sci* 122: 1963-1969.

GURSKAYA N G, VERKHUSHA V V, SHCHEGLOV A S, STAROVEROV D B, CHEPURNYKH T V, FRADKOV A F, LUKYANOV S and LUKYANOV K A (2006). Engineering of a monomeric green-to-red photoactivatable fluorescent protein induced by blue light. *Nat Biotechnol* 24: 461-465.

ITO K and MCGHEE J D (1987). Parental DNA strands segregate randomly during embryonic development of *Caenorhabditis elegans*. *Cell* 49: 329-336.

ITO K, MCGHEE J D and SCHULTZ G A (1988). Paternal DNA strands segregate to both trophectoderm and inner cell mass of the developing mouse embryo. *Genes Dev* 2: 929-936.

KIMURA H and COOK P R (2001). Kinetics of core histones in living human cells: little exchange of H3 and H4 and some rapid exchange of H2B. *J Cell Biol* 153: 1341-1353.

KIPREOS E T (2005). *C. elegans* cell cycles: invariance and stem cell divisions. *Nat Rev Mol Cell Biol* 6: 766-776.

LEE K K, GRUENBAUM Y, SPANN P, LIU J and WILSON K L (2000). *C. elegans* nuclear envelope proteins emerin, MAN1, lamin, and nucleoporins reveal unique timing of nuclear envelope breakdown during mitosis. *Mol Biol Cell* 11: 3089-3099.

MAYER W, NIVELEAU A, WALTER J, FUNDELE R and HAAF T (2000a). Demethylation of the zygotic paternal genome. *Nature* 403: 501-502.

MAYER W, SMITH A, FUNDELE R and HAAF T (2000b). Spatial separation of parental genomes in preimplantation mouse embryos. *J Cell Biol* 148: 629-634.

OOI S L, PRIESS J R and HENIKOFF S (2006). Histone H3.3 variant dynamics in the germline of *Caenorhabditis elegans*. *PLoS Genet* 2: e97.

OSWALD J, ENGEMANN S, LANE N, MAYER W, OLEK A, FUNDELE R, DEAN W, REIK W and WALTER J (2000). Active demethylation of the paternal genome in the mouse zygote. *Curr Biol* 10: 475-478.

SAMSON M, JOW M M, WONG C C, FITZPATRICK C, ASLANIAN A, SAUCEDO I, ESTRADA R, ITO T, PARK S K, YATES J R 3RD *et al.,* (2014). The specification and global reprogramming of histone epigenetic marks during gamete formation and early embryo development in *C. elegans*. *PLoS Genet* 10: e1004588.

SANTOS F, HENDRICH B, REIK W and DEAN W (2002). Dynamic reprogramming of DNA methylation in the early mouse embryo. *Dev Biol* 241: 172-182.

SCHONEGG S, HYMAN A A and WOOD W B (2014). Timing and mechanism of the initial cue establishing handed left-right asymmetry in *Caenorhabditis elegans* embryos. *Genesis* 52: 572-580.

SINGH D and POHL C (2014). Coupling of rotational cortical flow, asymmetric midbody positioning, and spindle rotation mediates dorsoventral axis formation in *C. elegans*. *Dev Cell* 28: 253-267.

STIERNAGLE T (2006). Maintenance of *C. elegans*. In *WormBook*, (Ed. COMMUNITY, T. C. E. R.), vol. doi/10.1895/wormbook.1.101.1, pp.1-11.

STRICKFADEN H, ZUNHAMMER A, VAN KONINGSBRUGGEN S, KÖHLER D and CREMER T (2010). 4D chromatin dynamics in cycling cells: Theodor Boveri's hypotheses revisited. *Nucleus* 1: 284-297.

SULSTON J E, SCHIERENBERG E, WHITE J G and THOMSON J N (1983). The embryonic cell lineage of the nematode *Caenorhabditis elegans*. *Dev Biol* 100: 64-119.

THOMSON I, GILCHRIST S, BICKMORE W A and CHUBB J R (2004). The radial positioning of chromatin is not inherited through mitosis but is established de novo in early G1. *Curr Biol* 14: 166-172.

WALTER J, SCHERMELLEH L, CREMER M, TASHIRO S and CREMER T (2003). Chromosome order in HeLa cells changes during mitosis and early G1, but is stably maintained during subsequent interphase stages. *J Cell Biol* 160: 685-697.

ZEISER E, FROKJAER-JENSEN C, JORGENSEN E and AHRINGER J (2011). MosSCI and Gateway compatible plasmid toolkit for constitutive and inducible expression of transgenes in the *C. elegans* germline. *PLoS One* 6: e20082.

Methods xxx (2015) xxx–xxx

Contents lists available at ScienceDirect

Methods

journal homepage: www.elsevier.com/locate/ymeth

Quantitative gene expression analysis in *Caenorhabditis elegans* using single molecule RNA FISH

Jitka Bolková, Christian Lanctôt *

Institute of Cellular Biology and Pathology, First Faculty of Medicine, Charles University in Prague, Albertov 4, 128 00 Prague, Czech Republic

ARTICLE INFO

Article history:
Received 14 September 2015
Received in revised form 6 November 2015
Accepted 8 November 2015
Available online xxxx

Keywords:
Gene expression
Single molecule analysis
RNA FISH
C. elegans
Image analysis
Nascent transcription

ABSTRACT

Advances in fluorescent probe design and synthesis have allowed the uniform *in situ* labeling of individual RNA molecules. In a technique referred to as single molecule RNA FISH (smRNA FISH), the labeled RNA molecules can be imaged as diffraction-limited spots and counted using image analysis algorithms. Single RNA counting has provided valuable insights into the process of gene regulation. This microscopy-based method has often revealed a high cell-to-cell variability in expression levels, which has in turn led to a growing interest in investigating the biological significance of gene expression noise. Here we describe the application of the smRNA FISH technique to samples of *Caenorhabditis elegans*, a well-characterized model organism.

© 2015 Published by Elsevier Inc.

1. Introduction

Most of the investigations aimed at determining gene activity have been carried out using methods such as microarray analysis or RNA-seq, which provide averaged expression levels in cell populations. This over-reliance on ensemble approaches has obscured the cell-to-cell variability (i.e. the noise) that could be observed when the expression analysis was performed in individual cells. Recently, however, single cell techniques have gained in popularity and are increasingly being used to study the biological significance of gene expression noise [1,2]. Among these, RNA FISH is unique in that it bypasses amplification steps and combines molecular hybridization and microscopy to reveal the localization of transcripts in complex cell populations or whole organisms. Advances in fluorescent probe design and synthesis have allowed the uniform *in situ* labeling of individual RNA molecules, which can be imaged as single spots and counted [3,4]. Single-RNA counting has revealed alternative modes of gene expression: constitutive transcriptional initiation or infrequent bursts of transcription. These modes have been associated with low and high cell-to-cell variability, respectively, and have been detected in a variety of models, including *Saccharomyces cerevisiae* [5], mammalian cell lines [6], embryonic stem cells [7] and *Drosophila* embryos [8]. The single molecule RNA FISH (smRNA FISH) method is constantly being improved. Recently, Shaffer et al. presented conditions (dubbed Turbo RNA FISH) that allow the whole procedure to be performed under 30 min [9] while Chen *et al.* developed a probe encoding scheme and an iterative hybridization/imaging procedure (called multiplexed error-robust FISH, MERFISH) that make it possible to detect up to 1000 RNA species in individual cells [10].

Caenorhabditis elegans is a small (~1 mm) roundworm that has become over the years a well-established model organism [11]. It develops according to an invariant lineage and comprises, among others, reproductive, digestive and excretory organs as well as muscles and a diffuse neural system. So far, relatively few published studies have taken advantage of the power of the smRNA FISH technique to analyze and to quantify gene expression in *C. elegans*. Those that did, however, provided novel and important insights into the gene regulation process in this model organism, and in particular in the control of gene expression variability [12,13]. It was found for instance that mutations in the *skn-1* gene, the master regulator of endodermal development, lead to stochastic fluctuations in the expression of downstream effector genes rather than to uniform inhibition and that this effect may explain the incomplete penetrance of such mutants [14]. In another report, Nair et al. showed by perturbing cell lineages and analyzing gene expression of developmental regulators that the onset of expression is coordinated with, but independent of cell divisions during early embryogenesis [15]. Finally, analysis of the expression of *lin-3* EGF and its Notch ligand targets by smRNA FISH revealed a global de-repression of the gene in mutants that affect the EGF/Ras pathway as well as an abrupt increase in the RNA counts for

* Corresponding author.
E-mail addresses: jitka.simandlova@lf1.cuni.cz (J. Bolková), clanctot9@hotmail.com (C. Lanctôt).

http://dx.doi.org/10.1016/j.ymeth.2015.11.008
1046-2023/© 2015 Published by Elsevier Inc.

Notch ligands in EGF-target cells during vulval induction [16,17]. These studies illustrate the power of performing quantitative gene expression analysis in a model organism for which a large collection of well-characterized mutants is available.

2. Overview of the method and main challenges

The smRNA FISH technique relies on the hybridization of well-defined sets of fluorescent probes to individual cellular RNAs in order to provide a quantitative measure of gene expression at the single cell level. Using this approach, single RNA molecules are turned into labeled diffraction-limited "dots" that can be imaged under the microscope and counted using image analysis algorithms [3,4]. Since smRNA FISH is a microscopy-based technique, it can be used to localize RNAs inside the cell, and in particular to distinguish between cytoplasmic and nuclear signals. The latter most often correspond to nascent transcripts. As a result of the loading of multiple polymerases on the template and limiting steps in the processing of pre-mRNA, the nuclear smRNA FISH dots usually represent multiple nascent transcripts that accumulate at the site of transcription and are thus more intense than their cytoplasmic counterparts. The RNA output at the site of transcription can be approximated from the intensity of the nuclear signal, thereby enabling one to assess the respective contribution of nascent transcription and steady state distribution to the overall RNA counts.

The smRNA FISH technique was pioneered by the groups of Tiagy and van Oudenaarden [6,18]. It consists of 6 main steps: sample preparation, fixation, hybridization, washes, imaging and signal quantification (Fig. 1). One of the main features of smRNA FISH is the use of homogeneously labeled oligonucleotide probes, which ensures efficient penetration, low background and reproducible signal strength. Amplification of the signal occurs through the use of up to 48 oligonucleotide probes against a given RNA target. As will be described below, the fact that the hybridization signals are similar to each other in terms of size and intensity is exploited by the image analysis algorithms to differentiate true and false positives.

Protocols have already been published to perform smRNA FISH in *C. elegans* [19]. The present paper presents improvements along four lines: (1) facilitated and gentler manipulation of samples through the use of "baskets" to transfer worms from one solution to the next; (2) acetone fixation of adult worms to reduce autofluorescence caused by aldehyde fixation; (3) shorter hybridization time; and (4) use of a mounting medium that is compatible with oil immersion objectives to improve imaging. It is important to mention here some of the drawbacks of the smRNA FISH technique. First, the throughput is currently limited to a few genes at a time, although recent advances have allowed the detection of 1001 different RNA species using a 14-bit probe encoding scheme, with a positive identification rate of 73% [10]. Second, in the case of highly expressed genes, the fluorescent signals from the individual RNA molecules can overlap, thus hindering their proper identification and leading to an underestimation of the RNA count. Super-resolution microscopy, in particular of the stochastic reconstruction variety such as STORM, could help to solve this problem of signal overlap; however, to our knowledge no report has yet appeared that combines super-resolution microscopy and smRNA FISH, and our own preliminary experience pointed out the inherent difficulties in acquiring STORM signals in 3D throughout the cell volume. Finally, the importance of being able to outline the cells of interest should not be underestimated if one wishes to quantify expression in single cells or to assess cell-to-cell variability in expression levels. While this usually proves not to be an issue when analyzing expression in mammalian cell cultures, it can create problems when attempting to analyze expression in complex tissues and whole organisms such as *C. elegans*. In these cases, it is necessary to devise a mean to identify single cells, usually via an additional fluorescent label such as membrane-targeted GFP or, as was done in a recent paper on vulval induction [20], by co-hybridization with probes against a gene that is known to be expressed in a well-defined subset of cells. Despite these shortcomings, smRNA FISH remains a powerful and reliable technique to investigate gene expression and regulation. In this paper, we describe its application to the study of these fundamental processes in the *C. elegans* model organism.

3. Material and reagents

Material

- Microscope slides, 76 mm × 26 mm × 1 mm, pre-cleaned, twin frosted end
- Coverslips, 18 mm × 18 mm, high quality #1.5
- Diamond pen
- Razor blade
- Metal block in dry ice: a block from a dry bath (e.g. 10 cm × 8 cm) is turned upside down, half-buried in pellets of dry ice and stored at −80 °C.
- Coplin jars
- Nitex nylon fabric, mesh size of 50 μm, manufactured by Sefar (cat. no. 03-50/37), purchased from Dominique Dutscher Inc. (cat. no. 074010)
- 24-well plate
- Parafilm
- Forceps
- 15-ml tube, polypropylene, conical bottom
- Glass tube with conical bottom, 17 × 112 mm
- Hybridization chambers: 13 mm diameter, 20 μl volume (Electron Microscopy Sciences Inc., cat. no. 70324-02)

Reagents

- Gelatin, from porcine skin (Sigma–Aldrich, cat. no. G1890)
- Chrome alum (Sigma–Aldrich, cat. no. 243361)
- 1 M sodium azide (NaN_3), Sigma–Aldrich S2002. *Caution*, this is a toxic substance.
- Poly-L-lysine (PLL) solution: heat 40 ml of ddH_2O (doubly-distilled water) to 60 °C. Dissolve 0.08 g of gelatin. Cool the solution to 37 °C. Add 0.008 g of Chrome Alum. Mix well. Add 40 μl of 1 M NaN_3 (final concentration is 1 mM). Dissolve 40 mg of poly-L-lysine (hydrobromide, M_w > 300 000 g/mol, Sigma–Aldrich, cat. no. P1524, final concentration is 1 mg/ml). Transfer to a 50-ml tube. Store at 4 °C.
- DEPC-treated ddH_2O: Dissolve 1 ml of diethyl pyrocarbonate (DEPC, Sigma–Aldrich, cat. no.D5758) per liter of ddH_20 under the hood. Mix until "oily droplets" have disappeared from the solution (15–30 min). Autoclave.
- 10 mM Tris–HCl pH 8, RNAse-free
- 10× PBS, RNAse-free: dissolve one PBS tablet (Sigma–Aldrich, cat. no. P4417) in 20 ml of DEPC-treated ddH_2O.
- 1× PBS, made in RNAse-free water
- Tween-20™, polyoxyethylene-sorbitan monolaurate, (Sigma–Aldrich, cat. no. P-5927)
- Methanol, in a Coplin jar, at −20 °C
- Acetone, at −20 °C
- 4% formaldehyde in 1× PBS: Add 10 ml of 16% formaldehyde (Electron Microscopy Sciences Inc., cat. no. 15710, EM grade) to 26 ml of DEPC-treated ddH_2O and 4 ml of 10× PBS RNAse-free.
- 0.5 mg/ml DAPI in 1× PBS, (Sigma–Aldrich, cat. no. 32670)

Please cite this article in press as: J. Bolková, C. Lanctôt, Methods (2015), http://dx.doi.org/10.1016/j.ymeth.2015.11.008

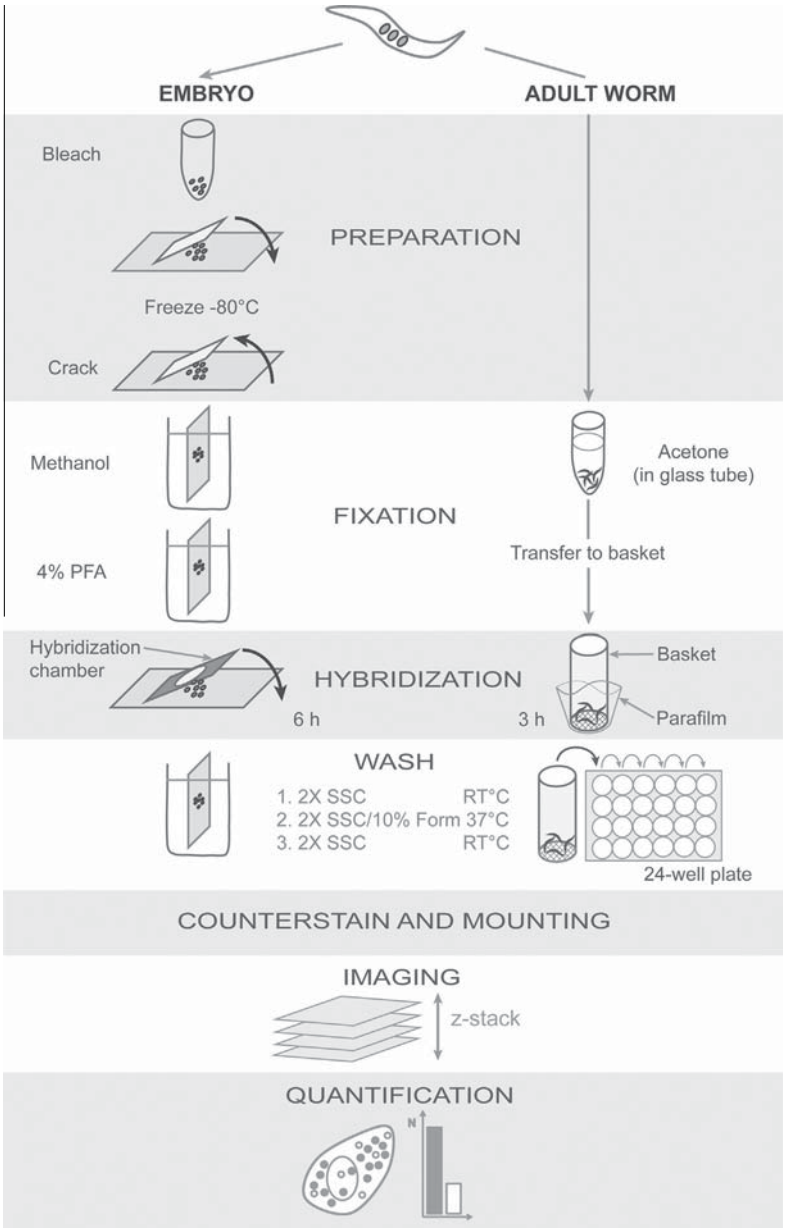

Fig. 1. Schematic outline of smRNA FISH on *C. elegans* samples. The procedure is performed either on slide for embryos and young larvae (left) or in suspension for L3 and L4 larvae and adult worms (right). The main steps are shown: preparation of samples, fixation, hybridization, washes, imaging and quantification. Apart from the way in which samples are handled (attached on slide or incubated in filter baskets), the main differences between the two protocols reside in (1) the need to freeze-crack samples on slide to allow penetration of reagents through the egg shell or cuticle; (2) the fixative that is used, i.e. 4% formaldehyde (PFA) for samples on slide and 100% cold acetone for those in suspension; (3) the shorter hybridization time for samples in suspension.

- Prolong Gold mounting medium, (Life Technologies, cat. no. 36934)
- 20× SSC, RNAse-free (Ambion/Life Technologies, cat. no. AM9763)
- Formamide, molecular biology grade, (Sigma–Aldrich, cat. no. 47674)
- 2× SSC/10% formamide: Add 5 ml of 100% formamide to 5 ml of 20× SSC and complete to 50 ml with DEPC-treated ddH_2O. Store at room temperature.
- 2× Hybridization buffer: dissolve 1 g of dextran sulfate (Sigma–Aldrich, cat. no. D8906) in 2 ml ddH_2O, add 200 µl of 10% BSA (w/v, prepared in DEPC-treated ddH_2O) and 1 ml 20× SSC RNAse-free and complete to 5 ml by DEPC-treated ddH_2O. Store at −20 °C.
- 200 mM ribonucleoside-vanadyl complex, (NEB cat.no. S1402S)
- 10 mg/ml yeast tRNA, (Sigma-Aldrich, cat. no. R5636)
- Wetting solution for tips and plastic Pasteur pipettes: 0.02% (v/v) Tween-20™ in DEPC-treated ddH_2O

4. Detailed protocol

4.1. Probe design and synthesis

The preferred probes are 20-mer oligonucleotides carrying a single fluorophore at one end (5′ or 3′). The small size of the probes (~6.5 kDa) allows for rapid and efficient penetration into the worm. To achieve a sufficient signal-to-background ratio, multiple probes are targeted along an individual RNA sequence. In our experience, a set of 36-48 probes that cover the entire length of the RNA

molecule provides an optimal signal strength. The probes are designed as follows.

1. Search for the gene of interest in Wormbase (www.wormbase.org).
2. Extract the sequence of the mature transcript using the view spliced + UTR function of the Page Contents – Sequences feature.
3. Paste the transcript sequence into the Stellaris RNA FISH probe designer on the website of the Biosearch Technologies company (https://www.biosearchtech.com/stellarisdesigner/). Choose *C. elegans* as organism and 3 as masking level. Use the default settings for maximum number of probes (48), length (20-mer) and spacing between probes (2 nt).
4. BLAST the recommended probes against the *C. elegans* genome. Discard the probes that show an aligned sequence of 16 nucleotides or more to an off target. Replace them by shifting the initial sequence a few nucleotides downstream or upstream along the target sequence and re-analyzing the resulting probe. Make sure that the chosen sequence retains a GC contents that is comparable to that of the other probes.

We routinely order sets of fluorescent oligonucleotides from commercial sources (e.g. Biosearch Technologies, Petaluma, CA, USA). These are labeled at the 3′ end. In our hands, the Quasar dyes perform best. The pooled oligonucleotides are resuspended to a final concentration of 25 μM in RNAse-free 10 mM Tris–HCl pH 8 and stored protected from light at −20 °C.

Notes

- In the rare event of an exceptionally long mature RNA (>4 kb), we use the last 3 kb of the transcript as target sequence. In *C. elegans*, the untranslated sequences are usually short and the majority of the probes therefore target the coding sequence.
- Alternatively, individual oligonucleotides can be synthesized with one aminoallyl derivative (C6-dT) at the 5′ end or up to one such modified nucleotide every ~10 bases. Theses oligonucleotides can then be labeled *in vitro* with amine-reactive fluorophores (e.g. N-hydroxysuccinimidyl-ester conjugates). After labeling, the oligonucleotides must be separated from the free dye molecules by size-exclusion chromatography. While this in-house labeling approach offers the flexibility of changing the fluorophore as needed, it is more time-consuming and less controlled than purchasing oligonucleotides that are labeled during synthesis.

4.2. Hybridization on slide

The hybridization procedure can be carried out either on a microscope slide or in suspension. However, in practical terms, older larvae (L3, L4) and adult worms attach poorly onto glass slides and it is therefore highly advisable to perform the hybridization of these samples in suspension, as described in Section 4.3. On the contrary, smRNA FISH on embryos and early larvae (L1, L2) is best carried out on samples that are attached to a microscope slide.

4.2.1. Treatment of slides

It is crucial to treat the slides in order to promote adhesion of the embryos and/or young larvae. The importance of this step cannot be overstated. To minimize loss of the sample, slides are coated with high molecular weight poly-L-lysine, which provides a positive surface to which the negatively charged egg shell/cuticle of the worm can attach.

1. Bring the poly-L-lysine (PLL) solution to room temperature.
2. Incubate two pre-cleaned microscope slides back-to-back in the PLL solution for 2 min.
3. Remove the slides from the PLL solution and place them upright against a support. Leave to dry at least 20 min, protected from dust.
4. Use on the same day.

Notes

- When stored at 4 °C, the PLL solution is stable for at least 2-3 months. It can be used repeatedly. However, it should be made fresh once a decrease in the adhesion of the samples to the slides is noticed.
- To provide even greater adhesiveness, a small drop of the PLL solution (~20 μl) can be pipetted in the center of the slide, which is then placed on a hot plate (~80 °C) and left there until the PLL solution has evaporated. The spot of evaporated PLL should be sticky.

4.2.2. Sample preparation and fixation

Samples are fixed by aldehyde crosslinking to optimally preserve cellular structure and morphology. Since the egg shell and the cuticle are impermeable to the fixative, a procedure referred to as 'freeze crack' (steps 5–7 below) is used to tear off part of these structures [21].

1. Isolate embryos or synchronized larvae according to standard procedures (see *Notes*).
2. Wash once in ddH_2O and resuspend in 50 μl of ddH_2O per starting 60 mm petri.
3. Label a PLL-treated slide. Using a diamond pen, slightly etch a circle of ~1 cm in diameter on the reverse side.
4. Deposit 25 μl of embryo/larva in the marked circle onto the PLL-treated microscope slide.
5. Gently cover with a 18 mm × 18 mm coverslip. Adsorb the excess liquid with a filter paper until the sample is slightly compressed.
6. Place the slide on a metal block in dry ice. Incubate at least 30 min at −80 °C.
7. Working rapidly, hold the slide vertically, insert a razor blade under the corner of the coverslip and pop it off.
8. Immediately fix the samples in cold methanol, 2 min at −20 °C. (The incubations in this and subsequent steps are performed in Coplin jars.)
9. Quickly dip the slides a few times in *cold* PBS. Transfer to *cold* 4% formaldehyde in PBS. Fix 10 min at room temperature.
10. Wash twice 3 min in fresh PBS at room temperature.
11. Equilibrate the slides in 2× SSC/10% formamide for at least 15 min and no longer than 1 h.

Notes

- Embryos are isolated by bleaching young gravid hermaphrodites [22]. Embryos are either used immediately or seeded on agar with food and left to develop until the desired stage.
- Worms and embryos tend to stick to plastic tips. To prevent loss of material, the tips should first be rinsed in a solution that contains traces of detergent (e.g. 0.02% Tween-20™) before pipetting the sample.
- The PBS and formaldehyde solutions that are used after the brief methanol fixation (step 9) must be cooled to 4 °C in ice or in the refrigerator before use. This pre-cooling step is important in order to avoid detachment of the samples from the slides.
- Before "cracking", the samples can be stored at −80 °C for up to a few days.

4.2.3. Hybridization, washes and mounting

1. For each sample, prepare the following mix (first dilute an aliquot of the probe 1:20 to 1.25 μM):

Probe(s) (1.25 μM)	1 μl
DEPC-treated ddH_2O	6.75 μl
10 mg/ml yeast tRNA	1 μl (optional)
200 mM ribonucleoside-vanadyl complex	1.25 μl (optional)
Formamide	2.5 μl

2. Add 12.5 μl of 2× Hybridization buffer. Mix well by vortexing. The final probe concentration is 50 nM and that of formamide, 10%.
3. Pipette 20 μl of the hybridization mix in a 13-mm hybridization chamber.
4. Take out a slide from the 2× SSC/10% formamide solution and carefully wipe out as much liquid as possible around the sample. Invert on the 20 μl drop in the hybridization chamber. Press gently to seal the hybridization chamber.
5. Hybridize at 37 °C for 6 h.
6. Remove the hybridization chamber and wash slides twice in 2× SSC for 5 min at room temperature.
7. Wash once in pre-heated 2× SSC/10% formamide for 30 min at 37 °C, occasionally pulling the slides out and back in.
8. Rinse in 2× SSC and wash once in 2× SSC for 5 min at room temperature.
9. Submerge the sample with 500 μl of 1 μg/ml DAPI. Stain for 2 min.
10. Rinse with 2× SSC and mount in Prolong Gold medium. Cure at least 24 h, seal with nail polish and proceed to imaging.

Notes

- The yeast tRNA and the ribonucleoside-vanadyl complex are added to the hybridization mix to protect cellular RNA from degradation.
- We find little difference in signal for probe concentrations ranging from 50 nM to 250 nM.
- In our hands, the Prolong Gold mounting medium consistently gives excellent results with cyanine or Quasar dyes.

4.3. Hybridization in suspension

As mentioned above, late larvae and adult worms do not attach well enough to the glass slide to withstand the smRNA FISH procedure. Hybridization is therefore carried out in suspension. To obviate the need to pellet the worms by centrifugation before each change of solution, we are using small home-made 'filter baskets' to transfer the samples from one solution to the next. These baskets have a 50 μm mesh bottom to allow for the rapid and efficient exchange of solutions while ensuring retention of the sample. We have found that the use of these filter baskets greatly facilitates and accelerates the handling of *C. elegans* samples during smRNA FISH. In addition, the omission of repeated centrifugations appears to lead to better preservation of worm morphology.

4.3.1. Preparation of filter baskets

1. Cut a ~2 cm^2 piece of Nitex nylon fabric (mesh size of 50 μm). Cut a P1000 tip approximately 2 cm from the large opening.
2. Briefly flame the large opening of the P1000 tip. Stamp the melted plastic onto the piece of nylon membrane.
3. Check that the nylon membrane is firmly attached to the tip and, if so, trim it down.

4.3.2. Fixation of samples

We have found that fixing adult worms with acetone leads to decreased levels of auto-fluorescence when compared with results obtained on aldehyde fixed samples. In addition, the absence of crosslinking in alcohol-fixed mammalian cells has been shown to allow for much faster hybridization [9]. We found that the same is true of worms fixed with acetone. It should be mentioned, however, that acetone fixation leads to loss of GFP signal and is therefore incompatible with the use of a GFP-based reporter to delimit or label cells.

1. Collect the worms from at least one fully grown 60 mm petri and transfer to a 15-ml conical bottom glass tube.
2. Let the worms settle and wash twice with ddH_2O.
3. Remove as much liquid as possible. Pipette 4 ml of cold (−20 °C) acetone onto the worm pellet. Mix well. Fix 10 min at room temperature.
4. Pipette out 2 ml of acetone, taking care not to remove worms, and replace with an equal volume of PBS. Mix well. Incubate 2 min.
5. Pipette out 2 ml of the acetone/PBS mix and replace with an equal volume of PBS. Mix well. Incubate 2 min.
6. Using a P1000 pipette tip that has been rinsed in PBS containing traces of detergent, transfer the worm solution into a home-made filter basket.
7. Rinse the worms by putting the basket in 1.5 ml of PBS in a well of a 24-well plate.
8. Transfer the filter basket to another well containing 1.5 ml of PBS. Incubate for 5 min.
9. Transfer the filter basket to another well containing 1.5 ml of 2× SSC/10% formamide. Mix once by lifting the basket up and down. Equilibrate the worms in this solution for at least 15 min at room temperature under the hood.

Notes

- All embryos and the majority of L1 and L2 larvae pass through the mesh of the filter basket. Older larvae and adults are retained, albeit with varying efficiency. A significant loss of even the adult worms occurs when the worm population is first transferred to the basket (up to 50% of individuals). Afterwards, minor losses occur throughout the procedure. However, it should be emphasized that the easy handling and gentle manipulation that are afforded by the use of filter baskets largely compensate for the loss of part of the sample.
- Some worms tend to aggregate during acetone fixation. This does not cause any problem in subsequent steps.
- Filter baskets made from P1000 tips can stand upright in the wells of a 24-well plate, but not in larger wells.

4.3.3. Hybridization, washes and mounting

1. For each sample, prepare the following mix:

Probe(s) (25 μM)	1 μl
DEPC-treated ddH_2O	32 μl
10 mg/ml yeast tRNA	2 μl (optional)
200 mM ribonucleoside-vanadyl complex	5 μl (optional)
Formamide	10 μl

2. Add 50 µl of 2× Hybridization buffer. Mix well by vortexing. The final probe concentration is 250 nM and that of formamide, 10%.
3. Pick up the filter basket and remove as much of the remaining equilibration medium as possible (~200 µl) by aspirating *through the membrane bottom*.
4. Place the basket upright in the center of a piece of parafilm (~2 cm^2). Wrap the parafilm around the basket to seal the filter membrane.
5. Pipette the hybridization mix (100 µl) in the basket. Swirl gently to mix. Check under the microscope that the worms are in the hybridization mix. Cover the whole basket with parafilm to avoid drying of the hybridization mix.
6. Put the wrapped basket in a tube and hybridize at 37 °C for 3 h in a water bath.
7. Unwrap the basket from the parafilm and aspirate as much hybridization mix as possible *through the bottom of the membrane*.
8. For each sample, prepare the following wells in a 24-well plate: 5 wells with 2× SSC and 2 wells with 2× SSC/10% formamide. Pipette 1.5 ml in each well.
9. Perform the following washes by transferring the filter basket from one well to the other:

2× SSC	rinse	once
2× SSC	wash 5 min	twice
2× SSC/10% formamide	rinse	once
2× SSC/10% formamide	wash 30 min	once (at 37 °C)
2× SSC	rinse	once
2× SSC	wash 5 min	once

10. After the last wash, stain the worms for 2 min in 1 µg/ml DAPI in the 24-well plate. Rinse once in 2× SSC. Leave the basket in 2× SSC.
11. Using a pipette tip rinsed in 0.02% Tween-20, transfer the worms from the basket to a microtube. Let worms settle.
12. Using a finely pulled capillary and working under the stereomicroscope, aspirate the solution as completely as possible without taking in any of the labeled worms.
13. Resuspend the worms in 10 µl of Prolong Gold mounting medium. Using a rinsed pipette tip transfer to a microscope slide and cover with a #1.5 high quality 18 mm × 18 mm glass coverslip. Cure at least 24 h, seal with nail polish and proceed to imaging.

4.4. Imaging

We image samples on an Olympus IX71 wide field fluorescence microscope equipped with high numerical aperture 60× or 100× oil immersion objectives and a sensitive Andor Clara CCD camera. It is not recommended to use a confocal microscope to image smRNA FISH spots because the signals are much weaker on this type of instruments. As a source of light, we use a standard 100 W high pressure mercury vapor lamp. Although some smRNA FISH protocols recommend the use of oxygen-depleting water mounting medium to avoid bleaching [19], we have found that the ready-to-use Prolong Gold antifade mounting medium provides excellent image quality and photostability. Furthermore, its refractive index is closer to that of oil, which limits optical aberrations, a property that is especially important when imaging the relatively thick *C. elegans* samples (30–100 µm). The sample is scanned at intervals of 250 nm along the *z*-axis using a computer-controlled piezo stage. It should be noted that the short working distances of the 60× and 100× objectives do not allow to collect high quality images throughout the worm volume; it is therefore preferable to scan different individuals from different angles. A total of approximately 40–60 optical sections are acquired, from longer to shorter wavelengths in the case of multicolor experiments. The typical exposure time is 200 ms per optical section. Fig. 2 shows a longitudinal section of a L4 worm hybridized with two different probes and counterstained with DAPI. Individual RNA molecules can be clearly detected, in intestinal

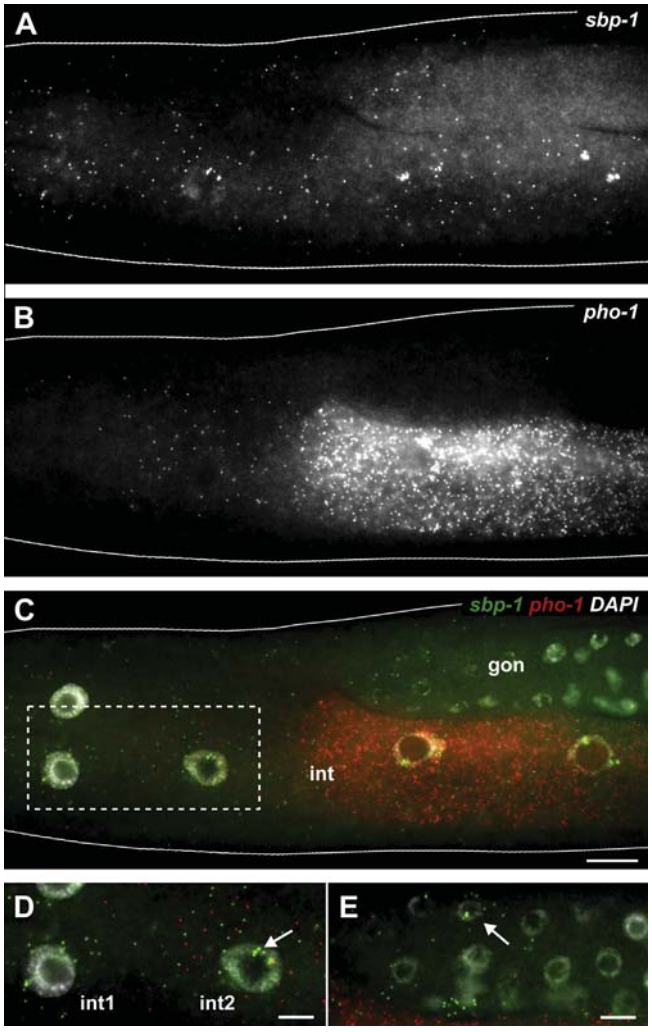

Fig. 2. Multicolor smRNA FISH results. The smRNA FISH procedure was carried out in suspension on L4 larvae and young adults, as described in the text. The probes that were used targeted the *sbp-1* or the *pho-1* gene products, and each consisted of pools of forty-eight 20-nt oligonucleotides labeled with Quasar 570 (green) or Quasar 670 (red), respectively. The nuclear DNA was counterstained with DAPI (gray). (A–C) The *sbp-1* signal alone, the *pho-1* signal alone and a merged pseudocolored image of both signals and the DAPI counterstain are shown in the anterior region of a L4 intestine and in the medial part of one of the gonads. The images are maximal projections of two consecutive optical sections (total thickness of 500 nm). In A and B, the brightness was adjusted to show single RNA dots in the cytoplasm. Boxed region in C is shown enlarged in panel D. int, intestine; gon, gonad. Scale bar, 10 µm. (D) *sbp-1* is expressed at similar levels in the two anteriormost segments of the *C. elegans* intestine (green dots in int1 and int2). The single molecule sensitivity of the smRNA FISH technique allows the expression of *pho-1* to be detected in the int2 segment (red dots), which is not the case with histochemical staining and reporter assays [27]. *pho-1* does not appear to be expressed in int1. The individual cytoplasmic mRNA molecules are clearly detected. The brighter spots in the DAPI-stained nucleus (arrow) represent sites of nascent transcription. Scale bar, 5 µm. (E) The RNA counts for *sbp-1* appear highly variable from cell to cell in the L4 gonad. Shown is a maximal projection of two optical sections taken from the same worm as in C. The arrow points to a local accumulation of *sbp-1* RNAs (green dots) and to a nucleus that displays nascent transcription spots. Scale bar, 5 µm.

and germ line cells in this case. In addition, brighter spots corresponding to sites of nascent transcription can be seen in the nuclei.

As mentioned above, one of the challenges in performing quantitative single cell smRNA FISH on *C. elegans* samples is actually to be able to outline the individual cells to which RNA molecules should be assigned. Unlike cultured cells, cells in the worm adopt complex three dimensional shapes that can be difficult to delineate without label. We found that using a membrane-targeted GFP can help to identify individual cells. It should be noted however that performing hybridization in the presence of formamide, even at low concentration as in the present protocols, leads to a decrease in the strength of GFP signals.

4.5. Quantification of gene expression

A number of freely available programs have been developed to quantify smRNA FISH results, including the Aro Spot Finding Suite (http://labs.biology.ucsd.edu/rifkin/software.html), StarSearch (http://rajlab.seas.upenn.edu/StarSearch/launch.html) and FISH-quant (https://code.google.com/p/fish-quant/). We are using the latter, which is a MATLAB-based software that can not only automatically count individual RNAs, but also process image stacks in batches and approximate the number of nascent transcripts at nuclear transcription sites [23]. Fig. 3 illustrates the initial step of the image analysis process, i.e. the generation of a filtered image which shows greatly increased signal-to-background ratio. It also shows that smRNA FISH signals having signal-to-background ratio as low as 1.3 on the untreated optical section can be efficiently converted to clear spots through filtering. Since cytoplasmic mRNA signals are diffraction-limited spots, the basic principle of the detection algorithm is to first identify local intensity maxima on the filtered image and then attempt to fit candidate spots with 3D Gaussian on the raw data. For each spot, quality scores which depend on the intensity of the surrounding pixels are calculated and are used after the detection and fitting steps to reject false positives.

The higher intensity of the RNA FISH signals and the co-localization with the DAPI signal are the distinctive features that usually allow nascent transcription spots to be identified. If needed, co-immunostaining for a component of the nuclear periphery, e.g. lamin B, can be used to rigorously assign smRNA FISH signals to either the nucleus or to the cytoplasm. To quantify nascent transcripts, we use the point-spread-function (PSF) superimposition approach, one of four that were built in the FISH-quant program. The PSF is the three-dimensional diffraction pattern produced by an infinitely small dot of light. The PSF superimposition approach first consists in generating an average PSF image from hundreds to thousands of cytoplasmic mRNAs. This average image is then taken as representative of a single RNA molecule and superimposed iteratively onto itself until the resulting image is more or less of the same size and intensity as the spot of nascent transcription, i.e. until the diffraction pattern of the reconstructed image is similar to that of the transcription spot. The number of iterations corresponds to the approximate number of nascent transcripts. This approach has the advantage of being able to take into account irregularly-shaped transcription spots. It is important to stress

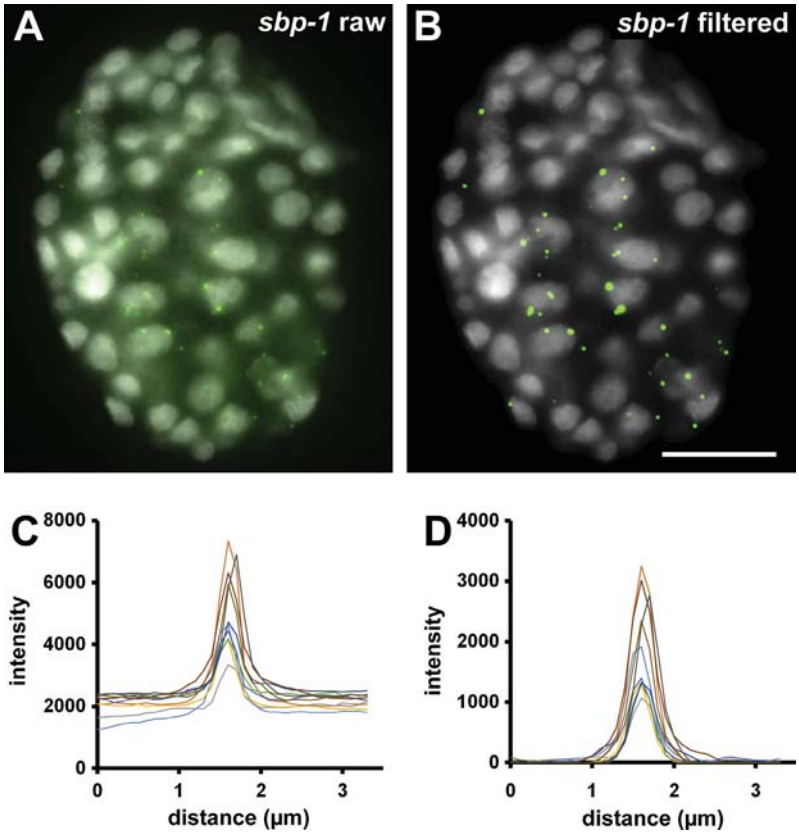

Fig. 3. Filtering smRNA FISH images to enhance spot detection. The smRNA FISH procedure was carried out on *C. elegans* embryos attached to a microscope slide, as described in the text. The probe targeted *sbp-1* transcripts and was labeled with Quasar-570 dye. The *sbp-1* (sterol regulatory element binding protein 1) gene is mainly expressed in the intestinal lineage. The images are maximal projections of four consecutive optical sections (total thickness of 1 μm). The nuclear DNA was counterstained with DAPI (gray). (A) A 117-cell embryo shows expression of *sbp-1* (green dots) in the putative E cells of the endodermal lineage. (B) Background removal is accomplished by subtracting a highly blurred image from the raw data and then enhancing spots in the resulting image using a low kernel Gaussian filter. This initial processing step leads to much better contrast. A total of 104 molecules are present in the embryo at the time of fixation. Scale bar, 10 μm. (C, D) Plots of pixel intensities measured for 10 spots along a 3.5 μm line centered on the spot. The data was extracted from the raw (C) or the filtered (D) images. Note the large increases in signal-to-noise ratio after filtering.

Please cite this article in press as: J. Bolková, C. Lanctôt, Methods (2015), http://dx.doi.org/10.1016/j.ymeth.2015.11.008

that, since the average image is generated from cytoplasmic RNA signals, the number of nascent transcripts that is computed is that of full-length equivalents. It can therefore easily be underestimated because the transcription spot comprises RNAs at different stages of synthesis, i.e. of different lengths, many of which will not hybridize with the complete set of oligonucleotide probes.

A useful indicator of cell-to-cell variability is the Fano factor, which is the variance of mRNA counts within a population over the mean count. If the Fano factor equals 1, then the mRNA counts follow a Poisson distribution, that is the probability of transcriptional initiation is constant over time. However, a Fano factor higher than 1 is indicative of transcriptional bursting, i.e. short periods of intense activity interspersed by periods of inactivity [3]. Measuring the proportion of cells that display labeled transcription sites in the cell nucleus and the output at each of these sites provides more direct information on the transcriptional dynamics of individual genes [24].

5. Concluding remarks

Here we described how to perform single molecule RNA FISH on *C. elegans* samples. smRNA FISH is a straightforward and powerful technique to analyze gene expression in this well-characterized model organism. Of note, the use of *C. elegans* allows one to study gene regulation in processes that can be difficult to faithfully reproduce in culture, such as gametogenesis, embryogenesis, disease development and aging [25,26]. In performing smRNA FISH experiments on *C. elegans* samples, special attention should be given to probe design to ensure specific coverage of the full-length mRNA molecule. In addition, care should be taken not to damage the embryos/worms during the procedure and to acquire the fluorescent signals with an objective of high quality and high numerical aperture combined with a sensitive CCD camera.

The main strength of the smRNA FISH approach is that it provides a quantitative view of gene expression in single cells, which often reveals high variability in expression levels between neighboring cells (see for instance the expression of *sbp-1* in the gonad, Fig. 2). The microscopy-based method further allows to focus on the quantification of expression at sites of nascent transcription inside the cell nucleus. Insights into the mode and dynamics of transcription can be inferred from the frequency and intensity of the nascent transcription spots. The stochastic nature of gene regulation has emerged as a research theme of broad interest in recent years, and no doubt the wider application of smRNA FISH to *C. elegans* biology will lead to novel discoveries in this field.

Disclosure of potential conflicts of interest

The authors indicate no potential conflicts of interest.

Acknowledgements

We gratefully acknowledge the financial support of the Czech Science Foundation (grants P305/12/1246 and P302/12/G157). This work was also partially supported by Charles University in Prague (PRVOUK P27/LF1/1). The Imaging Center at our institute is supported by the European Regional Development Fund (OPPK CZ.2.16/3.1.00/24010).

References

[1] Q. Deng, D. Ramskold, B. Reinius, R. Sandberg, Single-cell RNA-seq reveals dynamic, random monoallelic gene expression in mammalian cells, Science 343 (2014) 193–196.
[2] A. Sanchez, I. Golding, Genetic determinants and cellular constraints in noisy gene expression, Science 342 (2013) 1188–1193.
[3] A. Raj, A. van Oudenaarden, Single-molecule approaches to stochastic gene expression, Annu. Rev. Biophys. 38 (2009) 255–270.
[4] D.R. Larson, R.H. Singer, D. Zenklusen, A single molecule view of gene expression, Trends Cell Biol. 19 (2009) 630–637.
[5] D. Zenklusen, D.R. Larson, R.H. Singer, Single-RNA counting reveals alternative modes of gene expression in yeast, Nat. Struct. Mol. Biol. 15 (2008) 1263–1271.
[6] A. Raj, C.S. Peskin, D. Tranchina, D.Y. Vargas, S. Tyagi, Stochastic mRNA synthesis in mammalian cells, PLoS Biol. 4 (2006) e309.
[7] Z.S. Singer, J. Yong, J. Tischler, J.A. Hackett, A. Altinok, M.A. Surani, L. Cai, M.B. Elowitz, Dynamic heterogeneity and DNA methylation in embryonic stem cells, Mol. Cell 55 (2014) 319–331.
[8] A. Paré, D. Lemons, D. Kosman, W. Beaver, Y. Freund, W. McGinnis, Visualization of individual Scr mRNAs during *Drosophila* embryogenesis yields evidence for transcriptional bursting, Curr. Biol. 19 (2009) 2037–2042.
[9] S.M. Shaffer, M.T. Wu, M.J. Levesque, A. Raj, Turbo FISH: a method for rapid single molecule RNA FISH, PLoS ONE 8 (2013) e75120.
[10] K.H. Chen, A.N. Boettiger, J.R. Moffitt, S. Wang, X. Zhuang, Spatially resolved, highly multiplexed RNA profiling in single cells, Science 348 (2015) aaa6090.
[11] A.K. Corsi, B. Wightman, M. Chalfie, A transparent window into biology: a primer on *Caenorhabditis elegans*, Genetics 200 (2015) 387–407.
[12] I. Topalidou, A. van Oudenaarden, M. Chalfie, *Caenorhabditis elegans* aristaless/Arx gene alr-1 restricts variable gene expression, Proc. Natl. Acad. Sci. U.S.A. 108 (2011) 4063–4068.
[13] N. Ji, T.C. Middelkoop, R.A. Mentink, M.C. Betist, S. Tonegawa, D. Mooijman, H. C. Korswagen, A. van Oudenaarden, Feedback control of gene expression variability in the *Caenorhabditis elegans* Wnt pathway, Cell 155 (2013) 869–880.
[14] A. Raj, S.A. Rifkin, E. Andersen, A. van Oudenaarden, Variability in gene expression underlies incomplete penetrance, Nature 463 (2010) 913–918.
[15] G. Nair, T. Walton, J.I. Murray, A. Raj, Gene transcription is coordinated with, but not dependent on, cell divisions during *C. elegans* embryonic fate specification, Development 140 (2013) 3385–3394.
[16] A.M. Saffer, D.H. Kim, A. van Oudenaarden, H.R. Horvitz, The *Caenorhabditis elegans* synthetic multivulva genes prevent ras pathway activation by tightly repressing global ectopic expression of lin-3 EGF, PLoS Genet. 7 (2011) e1002418.
[17] J.S. van Zon, S. Kienle, G. Huelsz-Prince, M. Barkoulas, A. van Oudenaarden, Cells change their sensitivity to an EGF morphogen gradient to control EGF-induced gene expression, Nat. Commun. 6 (2015) 7053.
[18] A. Raj, P. van den Bogaard, S.A. Rifkin, A. van Oudenaarden, S. Tyagi, Imaging individual mRNA molecules using multiple singly labeled probes, Nat. Methods 5 (2008) 877–879.
[19] N. Ji, A. van Oudenaarden, Single molecule fluorescent in situ hybridization (smFISH) of *C. elegans* worms and embryos, in: The *C. elegans* Research Community, (Ed.), WormBook, 2012, http://dx.doi.org/10.1895/wormbook.1.7.1, pp. 1–16.
[20] M. Barkoulas, J.S. van Zon, J. Milloz, A. van Oudenaarden, M.A. Felix, Robustness and epistasis in the *C. elegans* vulval signaling network revealed by pathway dosage modulation, Dev. Cell 24 (2013) 64–75.
[21] S. Strome, W.B. Wood, Immunofluorescence visualization of germ-line-specific cytoplasmic granules in embryos, larvae, and adults of *Caenorhabditis elegans*, Proc. Natl. Acad. Sci. U.S.A. 79 (1982) 1558–1562.
[22] T. Stiernagle, Maintenance of *C. elegans*, in: The *C. elegans* Research Community (Ed.), Wormbook, 2006, Vol. doi/http://dx.doi.org/10.1895/wormbook.1.101.1, pp. 1–11.
[23] F. Mueller, A. Senecal, K. Tantale, H. Marie-Nelly, N. Ly, O. Collin, E. Basyuk, E. Bertrand, X. Darzacq, C. Zimmer, FISH-quant: automatic counting of transcripts in 3D FISH images, Nat. Methods 10 (2013) 277–278.
[24] K. Bahar Halpern, S. Tanami, S. Landen, M. Chapal, L. Szlak, A. Hutzler, A. Nizhberg, S. Itzkovitz, Bursty gene expression in the intact Mammalian liver, Mol. Cell 58 (2015) 147–156.
[25] R. Baumeister, L. Ge, The worm in us – *Caenorhabditis elegans* as a model of human disease, Trends Biotechnol. 20 (2002) 147–148.
[26] C. Gonzalez-Aguilera, F. Palladino, P. Askjaer, *C. elegans* epigenetic regulation in development and aging, Brief. Funct. Genomics 13 (2014) 223–234.
[27] T. Fukushige, B. Goszczynski, J. Yan, J.D. McGhee, Transcriptional control and patterning of the pho-1 gene, an essential acid phosphatase expressed in the *C. elegans* intestine, Dev. Biol. 279 (2005) 446–461.